Atmospheric Environment 45 (2011) 6317–6325

Contents lists available at SciVerse ScienceDirect

Atmospheric Environment

journal homepage: www.elsevier.com/locate/atmosenv

Trends in aerosol optical properties over the Bohai Rim in Northeast China from 2004 to 2010

Jinyuan Xin [a], LiLi Wang [a], Yuesi Wang [a,*], Zhanqing Li [b,1], Pucai Wang [a]

[a] State Key Laboratory of Atmospheric Boundary Layer Physics and Atmospheric Chemistry, Institute of Atmospheric Physics, Chinese Academy of Sciences, Beijing, 100029, PR China
[b] Department of Atmospheric & Oceanic Science, University of Maryland, College Park, MD 20782, USA

ARTICLE INFO

Article history:
Received 25 April 2011
Received in revised form
15 August 2011
Accepted 18 August 2011

Keywords:
Aerosol optical depth
Angstrom wavelength exponent
MODIS
Seasonal variation

ABSTRACT

Strong seasonal variations in regional aerosol optical depth at 550 nm (AOD) and aerosol type were investigated over China's Bohai Rim based upon six years' worth of data from four sites. Aerosol loading was higher and particle sizes were larger in the spring and summer than in the autumn or winter in the region. The regional mean background AOD and Angstrom exponent (α) were 0.20 ± 0.03 and 0.74 ± 0.17, respectively, and these values decreased by roughly 0.01 and 0.40 over the past six years. The annual mean AOD and α were 0.50 ± 0.06 and 1.09 ± 0.23 at three typical observation stations in the Bohai Rim economic zone. AOD increased by 0.07 and α decreased by 0.18 over the past six years, presumably due to rapid economic growth in the special zone. The accuracy of the MODIS C051 AOD product was relatively low over this region, and 52% of MODIS AOD product was within the expected error. The averaged standard deviation between annual mean ground-based and MODIS retrievals of AOD was ± 0.11, but the monthly mean and seasonal mean differences ranged from -0.34 to $+0.45$ and from -0.17 to $+0.24$, respectively, at the four sites studied. The calibrated MODIS AOD was adjusted by the seasonal liner regression functions between daily ground-observed AOD and raw MODIS AOD product. The averaged standard deviations of the calibrated MODIS AOD values were ± 0.02 for the annual means and ± 0.08 for the monthly means. The accuracy of the calibrated MODIS AOD was found to be reliable.

1. Introduction

During the past few decades, China has become one of the major factors in the uncertainty of aerosol climate and radiation effects on Earth due to dramatic increases in large-scale farming, urbanisation and industrial activities in this country (IPCC, 2007; Huebert et al., 2003; Li, 2004; Seinfeld et al., 2004). However, the spatial and temporal contributions of aerosol optical properties and aerosol types are very different over different regions in China. Large economic zones are emitting significant amounts of anthropogenic aerosols (Wang et al., in press; Lu et al., 2010). The Bohai Rim has become the third largest and most important economic zone in China after the Yangtze River Delta and the Pearl River Delta regions. It is located in northern China around the Bohai Sea and comprises several administrative districts. The Bohai Rim encompasses Beijing and Tianjin municipalities as well as part of Hebei, Liaoning and Shandong provinces. This area encompasses two municipalities, 24 prefecture level cities and 150 counties with a combined land area of 23.55×10^4 km^2 and a population measured at 120 million in 2010. This rapidly developing economic region, centered on Beijing and Tianjin, is thriving at an accelerated pace with industrialisation and urbanization (Guo et al., 2009).

Studies have shown that over the past decade, the amount and rates of emission of atmospheric pollutants and primary aerosols were highest in the Bohai Rim (Lu et al., 2010; Streets et al., 2003, 2004; Lei et al., 2011). Part of this growth is driven by new industry that consumes substantially more coal and fossil fuel in the region, releasing more absorbing soot and organic aerosols into the East Asian atmosphere (Lelieveld et al., 2001; Streets et al., 2001, 2003, 2004; Streets and Aunan, 2005). Aerosol optical properties are spatially and temporally inhomogeneous (Eck et al., 2005; Kim et al., 2007; Lu et al., 2010). Depending on aerosol type and meteorology, they may also be found far away from their sources (Levy et al., 2009). The aerosol optical depth (AOD) and Angstrom exponent (α) are fundamental aerosol properties that can be retrieved from ground-based sun photometer data and satellite data. Many researchers have investigated trends in aerosol optical

* Corresponding author. Tel.: +86 10 82080530.
E-mail addresses: xjy@mail.iap.ac.cn (J. Xin), wys@dq.cern.ac.cn, wys@mail.iap.ac.cn (Y. Wang).
[1] Also with: State Key Laboratory of Earth Surface Processes and Resource Ecology College of Global Change and Earth System Science, Beijing Normal University, PR China.

1352-2310/$ – see front matter © 2011 Elsevier Ltd. All rights reserved.
doi:10.1016/j.atmosenv.2011.08.052

properties based on satellite data (Mishchenko and Geogdzhayev, 2007a, Mishchenko et al., 2007b; Zhang and Reid, 2010; Zhao et al., 2008). However, averaged satellite products are highly dependent on choices made for data aggregation and weighting, and sampling errors can be further propagated when deriving regional or global mean AOD values (Levy et al., 2009, 2010; Remer et al., 2008; Li et al., 2009). This paper uses six years' worth of data to examine the spatial and temporal variability of aerosol optical properties along the Bohai Rim. The accuracy of Moderate Resolution Imaging Spectroradiometer (MODIS) AOD satellite-based retrievals over this prosperous economic region will also be assessed. Geographical information about the four sites and a description of data used in this study is given in Section 2. Results and discussion are presented in Section 3, and a summary is given in Section 4.

2. Observation sites and data

Fig. 1 shows the locations of the four sites under study in the Bohai Rim. The three Chinese Ecosystem Research Network stations (http://www.cern.ac.cn:8080/index.jsp) include Beijing Forest, Shenyang and Jiaozhou Bay. They are located in relatively remote areas so that large-scale regional background conditions of some typical ecosystems can be monitored. Note that these stations are part of the Chinese Sun Hazemeter Network (CSHNET) (Xin et al., 2007) established in 2004 under the East Asian Studies of Tropospheric Aerosols: An International Regional Experiment (EAST-AIRE) (Li et al., 2007). The stations are typical and representative for aerosol observation in different ecosystem regions (Wang et al., in press). The Beijing Forest ecosystem research station is situated on Donglingshan Mountain (39.97°N, 115.43°E, 1130 m elevation). A temperate semi-humid monsoon climate is typical for this site. The Shenyang station is located in the village of Shilihe (41.52°N, 123.63°E, 31 m elevation), which is surrounded by the extensive agricultural land. The Jiaozhou Bay marine ecosystem research station is located on the southeast shore of the Shandong peninsula (35.90°N, 120.18°E, 6 m elevation); it is a typical mid-sized, semi-enclosed bay. The Beijing City site (39.98°N, 116.37°E, 58 m elevation), a typical urban atmospheric observation station of Chinese Academy of Sciences, is located at the Institute of Atmospheric Physics in the northern outskirts of Beijing and has aerosol optical properties typical of urban areas. Hand-held LED hazemeters and Microtops II solar photometers were used to take measurements between 10 A.M. and 2 P.M. (local time), a period which overlapped with satellite overpass times. Measurements were taken during each observation period at times when a direct line of sight to the sun was present. Columnar AOD was estimated using the Beer–Lambert–Bouguer law. A log-linear curve fitting algorithm was applied to AODs at three wavelengths (405 nm, 500 nm and 650 nm) to estimate the Angstrom exponent (α) (Xin et al., 2007, 2006), a basic parameter related to the aerosol size distribution. In general, α values ranged from 0.0 to 2.0, with smaller values of α corresponding to larger aerosol particle sizes (Dubovik et al., 2002; Kim et al., 2004).

Fig. 1. Locations of the four sites in the Bohai Rim.

MODIS aerosol products were released to the public as 'Collection 003, 004, 005 (C003, C004, C005)' (Chu et al., 2002; Remer et al., 2005; Levy et al., 2007). The MODIS data used in this paper were the Collection 051 level 2 MOD04 aerosol product (with a 10 km*10 km resolution). Ground-based AODs at 550 nm were interpolated from AODs at 500 nm and 650 nm retrieved from hazemeter measurements. Hereafter, the acronym AOD means "aerosol optical depth at 550 nm", and the term "MODIS AOD" refers to the Collection 051 AOD product at 550 nm, if not specified otherwise. As the NASA research groups' suggestion (Ichoku et al., 2002; Chu et al., 2002; Remer et al., 2002), data matching was done in the following manner: if at least five pixels fell within a 50 km*50 km box centered on a sunphotometer site, the mean satellite-retrieved AOD was calculated. Ground-observed AOD was averaged within $\pm$0.5 h of the satellite overpass times. Observed AOD with standard deviation (SD) $>$ 0.5 was excluded to reduce validation errors.

3. Results and discussion

Table 1 summarises annual and seasonal mean values for ground-observed AOD values at 550 nm, Angstrom exponent (α), MODIS C051 AOD at 550 nm, the liner regression function and correlation coefficient of the daily observed AOD (x) and MODIS AOD (y) at four sites along the Bohai Rim.

3.1. The regional background site: Beijing Forest

Fig. 2a and b show a marked seasonal cycle in the monthly-averaged AOD and the monthly-averaged α from August 2004 to July 2010 at this site. The annual-averaged AOD was 0.20 with a standard deviation of 0.03, which was 2 times higher than the background continental AOD level of 0.10 (Holben et al., 2001; Eck et al., 2005). A maximum value for the ground-based retrieval of AOD (0.27) was found in the spring and summer, while α reached a minimum value of 0.47 during the summer. Seasonal cycles show that monthly mean AOD reached peak values (approximately 0.34) in May and June and that α reached its lowest value (approximately 0.39) in July (Fig. 2d). Dust storms and soil erosion are common during the transition from spring to summer, so the dominant aerosol types then are dust and soil aerosols (Zhou et al., 2004; Du et al., 2008; Xin et al., 2010a). In winter, the smallest and largest seasonal mean values of AOD and α were retrieved from ground-based measurements (0.13 and 1.18, respectively – see Table 1). The lowest mean aerosol loading ($\sim$0.11, close to the background level) was seen in November and December, while α reached its peak value ($\sim$1.59) in December (Fig. 2d). Fossil fuel and biomass burning generate more smoke and soot aerosols in the autumn and winter in northern China, and a gradual increase in snow and ice cover on the ground restricts the emission of coarse-mode mineral particles in the winter (Cao et al., 2005; Yan et al., 2006; Xin et al., 2007; Wang et al., in press).

Table 1
Annual and seasonal means and standard deviations of ground-based retrievals of observed AOD at 550 nm, Angstrom exponent (α), MODIS C051 AOD at 550 nm, linear regression function and correlation coefficient for daily observed AOD (x) and MODIS AOD (y) at four sites in the Bohai Rim.

	Site	Beijing Forest	Beijing City	Shenyang	Jiaozhou Bay
Annual mean	Observed AOD (x)	0.20 ± 0.03	0.48 ± 0.04	0.49 ± 0.07	0.54 ± 0.04
	MODIS AOD (y)	0.15 ± 0.03	0.62 ± 0.06	0.33 ± 0.02	0.51 ± 0.04
	Angstrom exponent, α	0.74 ± 0.17	1.09 ± 0.09	0.86 ± 0.27	1.26 ± 0.12
	Linear regression function	$y = 0.94x - 0.04$	$y = 1.07x + 0.11$	$y = 0.83x - 0.06$	$y = 0.97x - 0.02$
	Correlation coefficient, R^2	0.81	0.83	0.70	0.73
Spring	Observed AOD (x)	0.27 ± 0.09	0.60 ± 0.16	0.52 ± 0.13	0.64 ± 0.10
	MODIS AOD (y)	0.30 ± 0.07	0.74 ± 0.30	0.51 ± 0.14	0.73 ± 0.17
	Angstrom exponent, α	0.52 ± 0.19	0.98 ± 0.20	0.68 ± 0.26	1.08 ± 0.25
	Linear regression function	$y = 0.99x - 0.05$	$y = 1.13x + 0.16$	$y = 0.83x - 0.01$	$y = 1.14x - 0.05$
	Correlation coefficient, R^2	0.83	0.84	0.63	0.77
Summer	Observed AOD (x)	0.27 ± 0.12	0.61 ± 0.21	0.60 ± 0.16	0.80 ± 0.13
	MODIS AOD (y)	0.34 ± 0.15	0.85 ± 0.26	0.52 ± 0.19	0.73 ± 0.20
	Angstrom exponent, α	0.47 ± 0.24	1.14 ± 0.11	0.63 ± 0.26	1.08 ± 0.13
	Linear regression function	$y = 1.07x - 0.13$	$y = 0.98x + 0.19$	$y = 0.90x - 0.16$	$y = 0.87x - 0.03$
	Correlation coefficient, R^2	0.84	0.85	0.72	0.73
Autumn	Observed AOD (x)	0.15 ± 0.05	0.47 ± 0.12	0.40 ± 0.07	0.51 ± 0.10
	MODIS AOD (y)	0.17 ± 0.08	0.50 ± 0.17	0.31 ± 0.08	0.50 ± 0.11
	Angstrom exponent, α	0.90 ± 0.35	1.14 ± 0.16	1.00 ± 0.31	1.35 ± 0.15
	Linear regression function	$y = 0.89x - 0.04$	$y = 1.01x + 0.06$	$y = 0.77x - 0.06$	$y = 0.96x - 0.04$
	Correlation coefficient, R^2	0.79	0.83	0.75	0.75
Winter	Observed AOD (x)	0.13 ± 0.04	0.41 ± 0.09	0.37 ± 0.06	0.46 ± 0.08
	MODIS AOD (y)	0.11 ± 0.04	0.24 ± 0.06	0.28 ± 0.04	0.46 ± 0.08
	Angstrom exponent, α	1.18 ± 0.43	1.09 ± 0.17	0.96 ± 0.26	1.30 ± 0.18
	Linear regression function	$y = 0.70x + 0.02$	$y = 0.58 + 0.11$	$y = 0.61x + 0.07$	$y = 0.83x + 0.03$
	Correlation coefficient, R^2	0.60	0.71	0.58	0.69

Six years' worth of complete annual cycles of mean monthly AOD and α values at this site show some indication that AOD has decreased slightly over the years (by approximately 0.01 from 2004 to 2010) and that the particle size of the dominant aerosol has increased (mean α reduced from approximately 0.98 in 2004 to 0.58 in 2010). The "slight brightening" trend was consistent with global aerosol trends over the global and the oceans which the tropospheric AOT decrease over the 14-yaer period is estimated to be at least 0.02 (Mishchenko and Geogdzhayev, 2007a; Mishchenko et al., 2007b; Geogdzhayev et al., 2005). Whereas, neither AVHRR nor other existing satellite instruments can be used to determine unequivocally whether the recent AOT trend is due to long-term global changes in natural or anthropogenic aerosols (Mishchenko et al., 2007b).

Fig. 2c and d show that the raw MODIS AOD values expressed a similar seasonal variation but a different annual trend from ground-observed AOD measurements. Fig. 2e shows MODIS retrievals of AOD as a function of ground-based retrievals of AOD at the Beijing Forest site; the retrievals appear to agree relatively well (liner regression: $y = 0.94x - 0.04$, $R^2 = 0.81$). Of 669 valid MODIS/Beijing Forest co-located retrievals, 59% of them fell within NASA expected errors ($y = 0.05 + 1.15x$; $y = -0.05 + 0.85x$) during the six-year period. The averaged standard deviations of the MODIS AOD were ±0.10 for the daily means, ±0.08 for the monthly means and ±0.06 for the annual means. Seasonal break-downs of the liner regression functions are also presented in Table 1. AOD retrievals from MODIS were generally underestimated. By contrast, annual/seasonal (except for winter) mean and monthly mean (Fig. 2e) AOD retrievals from MODIS showed an overestimation. The percentages of MODIS/Beijing Forest co-located retrievals within the expected errors were 61% in the spring, 28% in summer, 54% in the autumn and 97% in winter. Fig. 2f shows how the MODIS AOD was calibrated using seasonal liner regression functions, and 86% of the calibrated MODIS AOD values fell within the NASA expected errors. The averaged standard deviations of the calibrated MODIS AOD were ±0.06 for the daily means, ±0.05 for the monthly means and ±0.01 for the annual means. These results imply that errors in MODIS AOD are mainly due to the surface reflectance, which has a large seasonal variation. Although MODIS retrievals of AOD can capture the seasonal variation in aerosol loading, they do not represent the background annual trend very well, except when calibrated using the ground-observed AOD.

3.2. The urban site: Beijing City

Fig. 3a and b show a regular seasonal cycle of AOD and α with large day-to-day variations over Beijing City (Eck et al., 2010; Yu et al., 2009), the largest city located along the Bohai Rim. The annual-averaged AOD from ground measurements was 0.48 ± 0.04. Although pollution is a serious problem in this city, large differences in aerosol loading and other components can occur, depending on the season and weather conditions (Guinot et al., 2007; Wang et al., 2009; Matsui et al., 2010). Maximum seasonal values were seen in the spring and summer (approximately 0.60) and in the winter, and a minimum AOD of 0.41 was found. Dust from urban activities and dust storms led to an increase in aerosol loading and particle size in the spring. Seasonal cycles (Fig. 3d) show that monthly mean AOD reached a peak value of 0.69 in April and that the monthly mean α reached a minimum value of 0.94 during that month also. Another peak in monthly mean AOD occurred in June (0.75), along with a peak in α (1.07), suggesting the generation of a second wave of aerosols with small particle sizes under higher ambient temperatures typical of the summer (Eck et al., 2010; Matsui et al., 2010; Xin et al., 2010b; Zheng et al., 2005). Annual and seasonal mean AOD values in Beijing City were greater than those in the Beijing Forest background site by approximately 0.28. Given that background AODs represented natural emission levels in the region, it was estimated that anthropogenic emissions and the generation of additional aerosols in the summer accounted for 58% of the aerosol load in Beijing City. There was unnoticeably week increase in monthly mean AOD from 2004 to 2010 (see Fig. 3a); during this period, a slight increase in

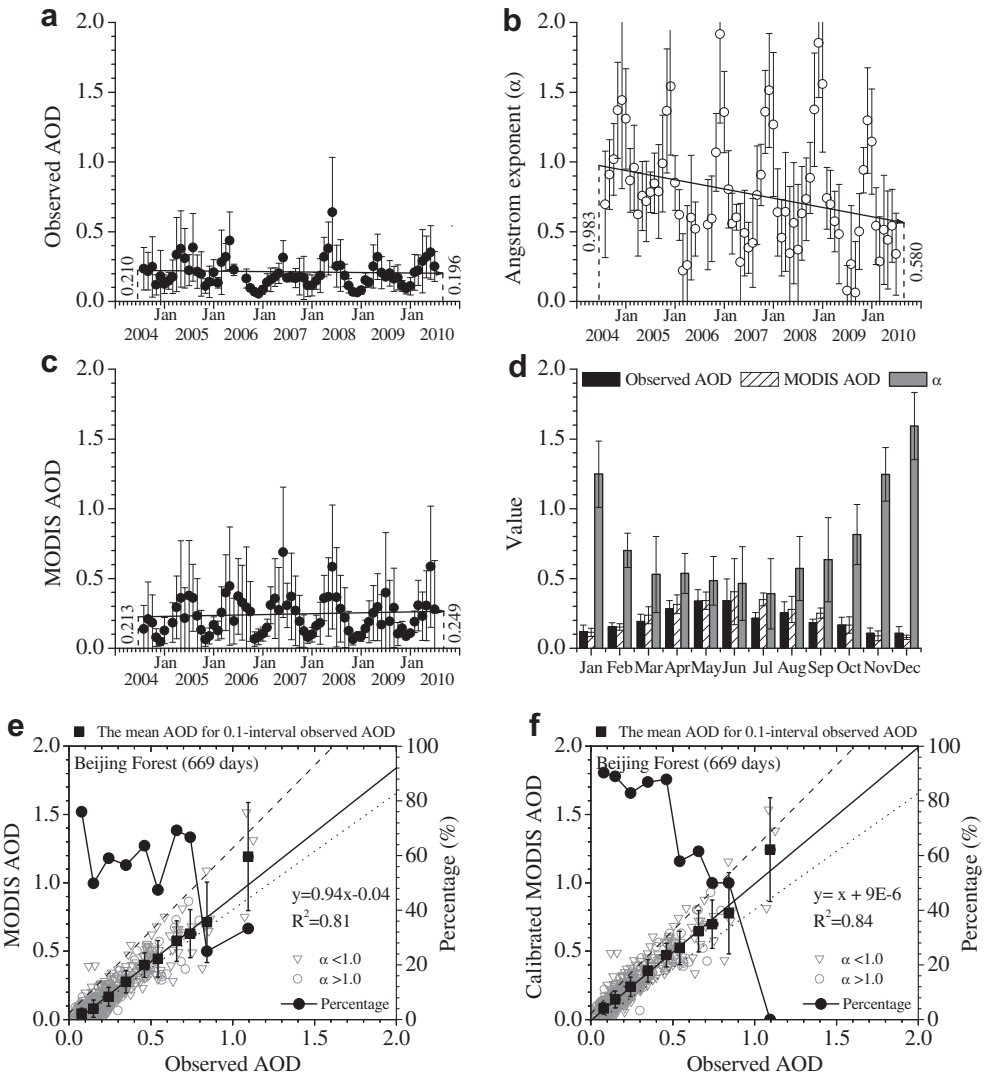

Fig. 2. Seasonal variations in the monthly-averaged observed AOD at 550 nm (a), Angstrom exponent (α) (b), MODIS C051 AOD at 550 nm (c), and their monthly change (d) at the Beijing Forest site. Comparisons of the MODIS retrievals of AOD against ground-based retrievals of AOD at 550 nm (gray circular and triangular symbols) (e) and the calibrated MODIS AOD against the observed AOD (f). The black square symbols are the observed and MODIS mean AODs binned over each 0.1-observed AOD increment; vertical and horizontal bars represent the standard deviations over each bin. Dashed lines represent $y = 0.05 + 1.15x$ and dotted lines represent $y = -0.05 + 0.85x$, which are the expected error lines reported by NASA. Filled circles represent the percentage of MODIS AODs falling within the expected error lines in each bin.

the monthly mean α was seen (see Fig. 3b). The results imply that the concentration of small aerosol particles (secondary compounds) increased over the six years.

Fig. 3c and d show that the raw MODIS AOD data demonstrated a similar seasonal variation and annual trend compared to ground-observed AOD. Fig. 3e shows a good correlation between MODIS and ground-based retrievals of AOD at Beijing City site (linear regression: $y = 1.07x + 0.11$, $R^2 = 0.83$) over the six-year period, but only 42% of the matched points fell within the area delineated by the linear relationships representing expected errors. The averaged standard deviations of the MODIS AOD were ±0.24 for the daily means, ±0.17 for the monthly means and ±0.15 for the annual means. The liner regression functions (Table 1) showed similar systematic deviation of the MODIS AOD values in all four seasons. The percentages of MODIS AOD retrievals falling within the expected error range for each season were 25% in the spring, 33% in the summer, 55% in the autumn and 81% in the winter. Considering all points (Table 1), AOD retrievals from MODIS in this urban region were overestimated. The annual mean MODIS-retrieved AOD (0.58) was greater than that of the ground-based retrieval of AOD (0.53), with seasonal (spring, summer, and autumn) overestimates of satellite AOD retrievals ranging from 0.03 to 0.24. In the winter, the mean MODIS-retrieved AOD (0.24) was less than the mean ground-based AOD retrieval (0.41). Fig. 3f shows how the MODIS AOD values were calibrated using the seasonal linear regression functions; 68% of the calibrated MODIS AOD values fell within the NASA expected errors. The averaged standard deviations of the calibrated MODIS AOD were ±0.11 for the daily means, ±0.10 for the monthly means and ±0.02 for the annual means. The mean standard deviation was ±0.11. These statistics imply that errors in the MODIS AOD were mainly due to the surface reflectance, which has a large seasonal variation at this urban site. In view of these large seasonal errors, the raw MODIS AOD values cannot adequately represent the annual trend in AOD in this urban area.

3.3. The agricultural site: Shenyang

Fig. 4a and b show the seasonal cycle of aerosol optical properties at the Shenyang site, located in the northern part of the

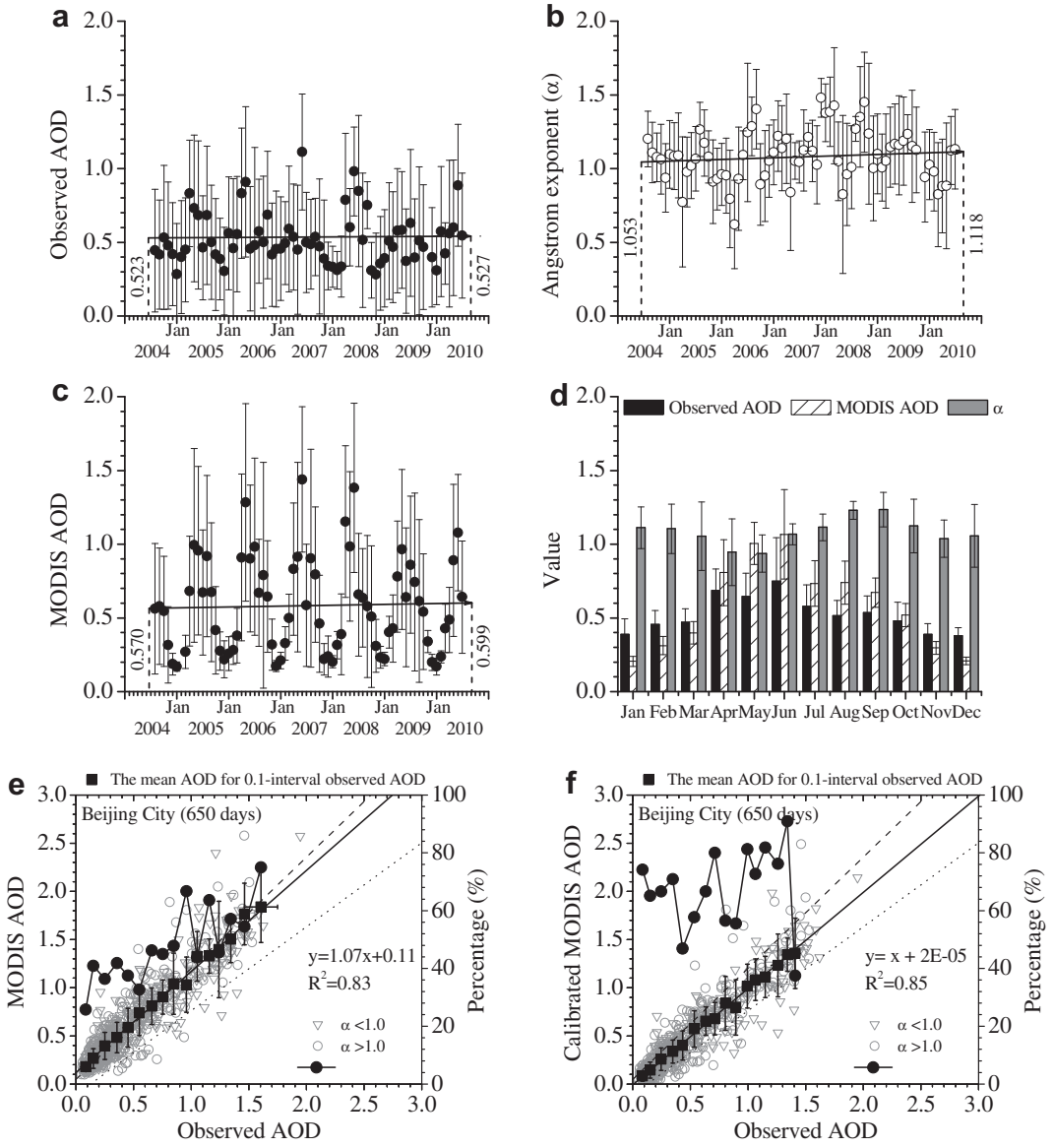

Fig. 3. Seasonal variations in the monthly-averaged observed AOD at 550 nm (a), Angstrom exponent (α) (b), MODIS C051 AOD at 550 nm (c), and their monthly change (d) at the Beijing City site. Comparisons of the MODIS retrievals of AOD against ground-based retrievals of AOD at 550 nm (gray circular and triangular symbols) (e) and the calibrated MODIS AOD against the observed AOD (f). The black square symbols are the observed and MODIS mean AODs binned over each 0.1-observed AOD increment; vertical and horizontal bars represent the standard deviations over each bin. Dashed lines represent $y = 0.05 + 1.15x$ and dotted lines represent $y = -0.05 + 0.85x$, which are the expected error lines reported by NASA. Filled circles represent the percentage of MODIS AODs falling within the expected error lines in each bin.

Bohai Rim. The annual mean ground-based retrievals of AOD and α were 0.47 and 0.82, respectively (see Table 1). The seasonal mean maximum AOD (0.60) and minimum α (0.63) occurred during the summer; the seasonal mean minimum and maximum values of AOD (0.37) and α (1.00) were seen in the winter and autumn, respectively. Fig. 4d shows that in June, the monthly mean ground-based retrieval of AOD reached a peak value of 0.68, and the monthly mean α reached a minimum value of 0.60. The aerosol type was continental in nature, due to dust storms and local soil emissions from farming practices during the transition from spring to summer (Xin et al., 2007). The monthly mean AOD reached a minimum value of 0.31 in December, and the monthly mean α reached its peak value of 1.12 during that month as well. Aerosol particle size decreased from autumn to winter, reflecting the agricultural practice of burning crop stalks in the autumn and the increase in fossil fuel and biomass burning for heating as the winter season approached (Cao et al., 2005; Yan et al., 2006). Meanwhile, a gradual increase in snow and ice cover on the ground prevented soil erosion and thus restricted the emission of coarse-mode mineral particles, a pattern that is also suggested by the low AOD loadings recorded in the winter (Xin et al., 2007). The time series of six years' worth of AOD retrievals shows a clearly increasing trend in monthly mean AOD values (Fig. 4a) and particle size of the dominant aerosols (Fig. 4b); from 2004 to 2010, monthly mean AOD increased from 0.38 to 0.55, and the monthly mean α decreased from 1.1 to 0.55. Revitalisation of old industrial sites has been underway since the beginning of the 21st century in Northeastern China. The rapid increase in industrial production and in construction has led to greater emissions of larger particles in the region (Zhang and Reid, 2010; Lu et al., 2010; Tian et al., 2005; Streets et al., 2004). This indicates the presence of anthropogenic aerosols associated with significant industrial

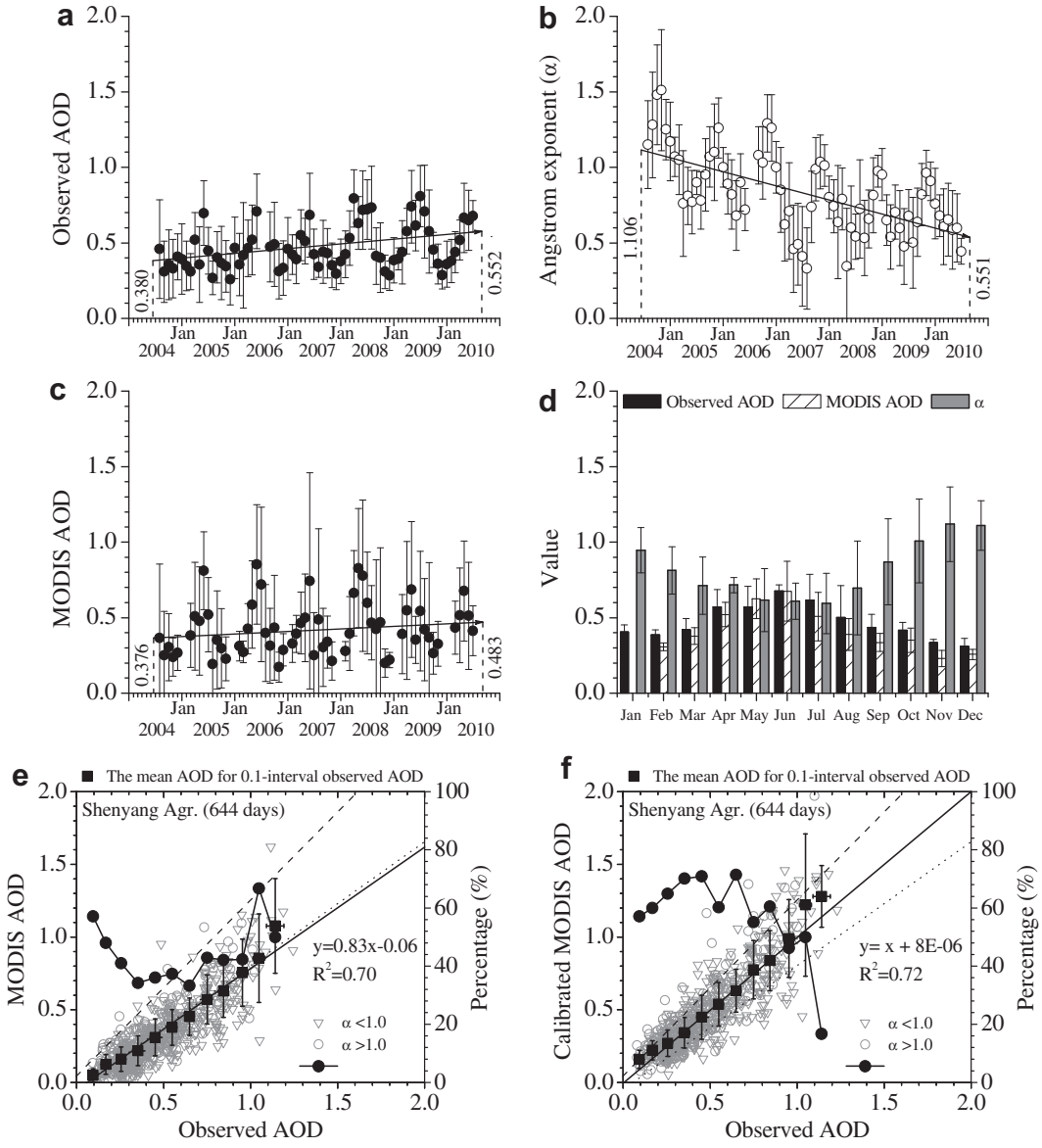

Fig. 4. Seasonal variations in the monthly-averaged observed AOD at 550 nm (a), Angstrom exponent (α) (b), MODIS C051 AOD at 550 nm (c), and their monthly change (d) at the Shenyang site. Comparisons of the MODIS retrievals of AOD against ground-based retrievals of AOD at 550 nm (gray circular and triangular symbols) (e) and the calibrated MODIS AOD against the observed AOD (f). The black square symbols are the observed and MODIS mean AODs binned over each 0.1-observed AOD increment; vertical and horizontal bars represent the standard deviations over each bin. Dashed lines represent $y = 0.05 + 1.15x$ and dotted lines represent $y = -0.05 + 0.85x$, which are the expected error lines reported by NASA. Filled circles represent the percentage of MODIS AODs falling within the expected error lines in each bin.

activity in the region. This increase causes a large variation in aerosol concentration and type and also increases the uncertainty of aerosol effects on regional climate change, e.g., on the regional precipitation and temperature (Menon et al., 2002; Duan and Mao, 2009).

Fig. 4c and d show that the raw MODIS AOD expressed similar seasonal variations and annual trends compared to ground-observed AOD. Fig. 4e shows MODIS retrievals of AOD as a function of ground-based retrievals of AOD at the Shenyang site; the retrievals agreed reasonably well (liner regression: $y = 0.83x-0.06$, $R^2 = 0.70$), and 40% of the matched points fell within the area delineated by the linear relationships representing expected errors. The averaged standard deviations of the MODIS AOD were ±0.20 for the daily means, ±0.17 for the monthly means and ±0.16 for the annual means. The liner regression functions (Table 1) showed similar systematic deviations of the MODIS AOD values in all four seasons. The percentages of MODIS AOD retrievals falling within the expected errors for each season were 54% in the spring, 20% in the summer, 30% in the autumn and 65% in the winter. Seasonal linear regression functions are presented in Table 1. Considering all points, mean AOD retrievals from MODIS in this agricultural region were generally underestimated, although during some months (e.g., March, April), mean AOD retrievals from MODIS were greater than those from ground-based measurements. Few MODIS data retrievals were reported in January and December because the surface reflectance was too large during these months due to snow and ice covering the ground. Fig. 3f shows how MODIS AOD was calibrated using seasonal linear regression functions; 64% of the calibrated MODIS AOD values fell within the NASA expected errors. The averaged standard deviations of the calibrated MODIS AOD were ±0.09 for the daily means, ±0.08 for the monthly means and ±0.04 for the annual means.

3.4. The maritime site: Jiaozhou Bay

Fig. 5a and b show the seasonal cycle of AOD and α at the Jiaozhou Bay site, located along the Shandong Peninsula in the southern part of the Bohai Rim. The annual mean ground-based retrievals of AOD and α were 0.54 $\pm$ 0.04 and 1.26 $\pm$ 0.12, respectively, suggesting a high concentration of small particles at this maritime site (Table 1). Rapid industrial development and human activities (such as farming, building and traffic) have led to increases in aerosol emissions, especially sulfate aerosols, along the eastern coastal area of China (Lu et al., 2010; Tian et al., 2005; Streets et al., 2004; Lei et al., 2011). The seasonal maximum of ground-based retrievals of AOD was 0.80 and occurred during the summertime, as did the seasonal minimum mean value of α (1.08). Fig. 5d shows that in July, the monthly mean ground-based retrieval of AOD reached a peak value of 0.86, and the monthly mean α reached a minimum value of 1.05. The transport of dust and continental pollution contributed to high aerosol loading and large particle sizes in the spring, while during the summer, massive emissions of hygroscopic sulfate aerosols and an abundance of water vapor led to a maximum in AOD and particle size (Han et al., 2010; Xiao et al., 1998; Sheng et al., 2005; Wang et al., in press). The seasonal minimum in ground-based retrievals of AOD was 0.46 in the winter, and the seasonal maximum of α was 1.35 in autumn. The monthly mean AOD reached a minimum value of 0.39 in December, and the monthly mean α reached its peak value of 1.40 during that month (Fig. 5d). Influxes of cold air and clean ocean air alternately washed atmospheric pollution out of the atmosphere and decreased AOD during the winter and fall seasons in this part of the Bohai Rim. The site is also under the influence of biomass and fossil fuel burning during autumn and winter, which produce heavy loadings of fine-mode aerosols. The time series of six years' worth of AOD retrievals shows a slight increasing trend in monthly mean AOD (Fig. 5a) and a slight decreasing trend in the particle size of the

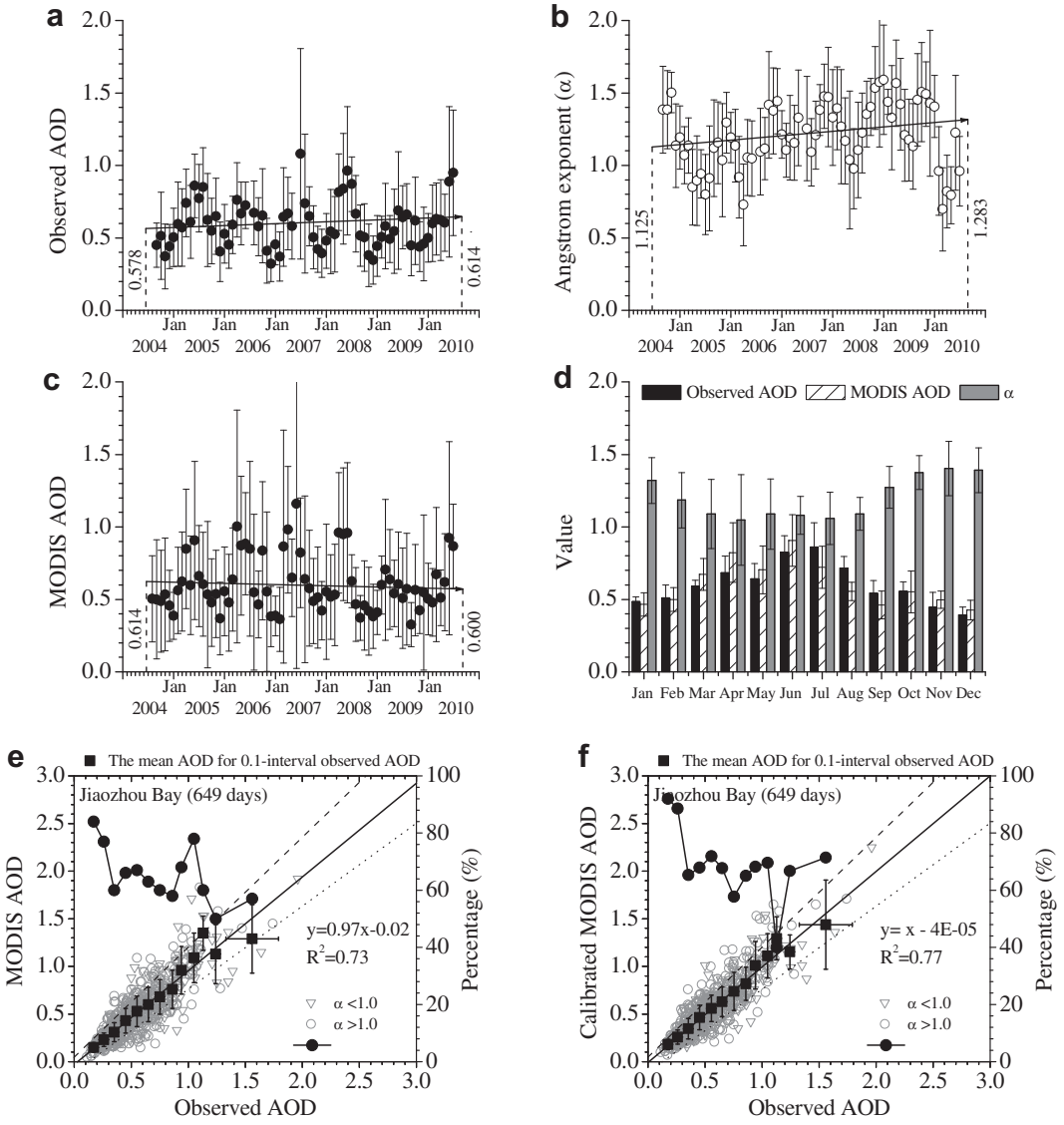

Fig. 5. Seasonal variations in the monthly-averaged observed AOD at 550 nm (a), Angstrom exponent (α) (b), MODIS C051 AOD at 550 nm (c), and their monthly change (d) at the Jiaozhou Bay site. Comparisons of the MODIS retrievals of AOD against ground-based retrievals of AOD at 550 nm (gray circular and triangular symbols) (e) and the calibrated MODIS AOD against the observed AOD (f). The black square symbols are the observed and MODIS mean AODs binned over each 0.1-observed AOD increment; vertical and horizontal bars represent the standard deviations over each bin. Dashed lines represent $y = 0.05 + 1.15x$ and dotted lines represent $y = -0.05 + 0.85x$, which are the expected error lines reported by NASA. Filled circles represent the percentage of MODIS AODs falling within the expected error lines in each bin.

dominant aerosol (Fig. 5b); from 2004 to 2010, the monthly mean AOD increased from 0.57 to 0.61, and the monthly mean α increased from 1.12 to 1.28. With the rapid development of industrialisation and modernisation, the emission of anthropogenic aerosols and the generation of secondary aerosols has increased in recent years over the Shandong Peninsula (Zhang and Reid, 2010; Lu et al., 2010; Tian et al., 2005; Streets et al., 2004). This observation is in agreement with the findings of significant increases in AOD along the East China Sea (Geogdzhayev et al., 2005) and the south-eastern coasts of Asia (Mishchenko and Geogdzhayev, 2007a), which be the expected result of rapidly growing regional economies coupled with the widespread use of technologies (Streets et al., 2006; Ohara et al., 2007).

The linear correlation equation ($y = 0.97x - 0.02$, $R^2 = 0.73$; Fig. 5e) shows that the accuracy of the satellite products was higher at Jiaozhou Bay than at the other sites. The annual mean MODIS and ground-based retrievals of AOD were almost the same (approximately 0.6). The averaged standard deviations of the MODIS AOD were $\pm$0.16 for the daily means, $\pm$0.10 for the monthly means and $\pm$0.04 for the annual means. The liner regression functions (Table 1) showed the similar systematic deviations of the MODIS AOD in all four seasons. The percentage of the data falling within the area delineated by the linear relationships representing expected errors was 66%. The percentages of MODIS AOD retrievals falling within the expected errors for each season were 71% in the spring, 51% in the summer, 61% in the autumn and 74% in the winter. In springtime, the mean MODIS-retrieved AOD was greater than the mean ground-based AOD retrieval by 0.09, and during the summer, the mean MODIS-retrieved AOD was less than the mean ground-based AOD retrieval by 0.07; both retrievals were the same in the autumn and winter months. Fig. 5f shows how MODIS AOD was calibrated using seasonal linear regression functions; 71% of the calibrated MODIS AOD values fell within the NASA expected errors. The averaged standard deviations of the calibrated MODIS AOD values were $\pm$0.10 for the daily means, $\pm$0.07 for the monthly means and $\pm$0.01 for the annual means. The accuracy of the calibrated MODIS AOD values was thus improved relative to the uncalibrated values.

4. Conclusions

Based on the above limited discussion the regional ground-based observation shows a “slight brightening” trend in the regional background AOD during the past six years, which was consistent with global aerosol trends over the global and the oceans (Mishchenko and Geogdzhayev, 2007a; Mishchenko et al., 2007b; Geogdzhayev et al., 2005). By contrast, there was a “dimming” trend in the Bohai Rim, where AOD showed a slight increase over the years. Mishchenko and Geogdzhayev (2007a) and Geogdzhayev et al. (2005) also investigated that high small aerosol loaded in the East China Sea. Urbanisation and industrialisation in economically expanding industrial areas has accelerated the emission of anthropogenic aerosols into the atmosphere and the generation of secondary aerosols. The rapid increases in commercial production and construction have led to emissions of larger aerosols over the northern part of the Bohai Rim. Given that the background AOD (0.20) represents the natural background level, anthropogenic emissions and secondary aerosol generation contribute approximately 0.30 to the aerosol loading in this region. This increase causes a large variation in aerosol concentration and type and also increases the uncertainty of aerosol effects on regional climate change.

In addition, the MODIS C051 AOD product can capture the seasonal variation of AOD in the region, but it cannot accurately represent aerosol trends. There are the complex terrains and landforms as well as the various ecological systems, including the mountain, the forest, the farmland, the shore, and the urban and suburban areas in the region. Especially, there are hundreds of small towns and cities, medium and large cities are scattered in the region like stars. The complex and various surfaces cause non-equivalent inversion errors of surface reflectance in the different seasons. Retrieval differences can be further propagated when deriving the monthly mean AOD, especially big differences in the summer and winter. Levy et al. (2009, 2010), Remer et al. (2008), and Li et al. (2009) also found the propagation of retrieval differences when deriving regional or global mean AOD values. MODIS products are quantitatively useful if their limitations and assumptions relative to ground-based measurements are taken into account.

Acknowledgments

This work was partially supported by the 863 Program (No. 2006AA06A303), the CAS Strategic Priority Research Program Grant No. XDA05100100, the public project of the Beijing Municipal Science & Technology Commission (D09040903670902), US Dept of Energy (DEFG0208ER64571), and NASA (NNX08AH71G). The authors are grateful to the Chinese Ecosystem Research Network (CERN) stations managed by the Chinese Academy of Sciences for their contribution to this research.

References

Cao, G., Zhang, X., Wang, D., Zheng, F., 2005. Inventory of atmospheric pollutants discharged from biomass burning in China continent. China Environmental Science 25 (4), 389–393 (in Chinese).

Chu, D.A., Kaufman, Y.J., Ichoku, C., Remer, L.A., Tanré, D., Holben, B.N., 2002. Validation of MODIS aerosol optical depth retrieval over land. Geophysical Research Letters 29 (12), 8007–8011.

Du, W., Xin, J., Wang, M., Gao, Q., Li, Z., Wang, Y., 2008. Photometric measurements of spring aerosol optical properties in dust and non-dust periods in China. Atmospheric Environment 42 (34), 7981–7987.

Duan, J., Mao, J.T., 2009. Influence of aerosol on regional precipitation in North China. Chinese Science Bulletin 54 (3), 474–483.

Dubovik, O., Holben, B.N., Eck, T.F., Smirnov, A., Kaufman, Y.J., King, M.D., Tanre, D., Slutsker, I., 2002. Variability of absorption and optical properties of key aerosol types observed in worldwide locations. Journal of the Atmospheric Sciences 59, 590–608.

Eck, T.F., Holben, B.N., Dubovik, O., Smirnov, A., Goloub, P., Chen, H.B., Chatenet, B., Gomes, L., Zhang, X.-Y., Tsay, S.-C., Ji, Q., Giles, D., Slutsker, I., 2005. Columnar aerosol optical properties at AERONET sites in central eastern Asia and aerosol transport to the tropical mid-Pacific. Journal of Geophysical Research 110, D06202.

Eck, T.F., Holben, B.N., Sinyuk, A., Pinker, R.T., Goloub, P., Chen, H., Chatenet, B., Li, Z., Singh, R.P., Tripathi, S.N., Reid, J.S., Giles, D.M., Dubovik, O., O'Neill, N.T., Smirnov, A., Wang, P., Xia, X., 2010. Climatological aspects of the optical properties of fine/coarse mode aerosol mixtures. Journal of Geophysical Research 115, D19205.

Geogdzhayev, I.V., Mishchenko, M.I., Terez, E.I., Terez, G.A., Gushchin, G.K., 2005. Regional advanced very high resolution radiometer–derived climatology of aerosol optical thickness and size. Journal of Geophysical Research 110, D23205.

Guinot, B., Cachier, H., Sciare, J., Tong, Y., Xin, W., Jianhua, Y., 2007. Beijing aerosol: atmospheric interactions and new trends. Journal of Geophysical Research 112, D14314.

Guo, L., Wang, D., Qiu, J., Wang, L., Liu, Y., 2009. Spatio-temporal patterns of land use change along the Bohai Rim in China during 1985–2005. Journal of Geographical Sciences 19, 568–576.

Han, X., Zhang, M.G., Han, Z.W., Xin, J.Y., Wang, L.L., Qiu, J.H., Liu, Y.J., 2010. Model analysis of aerosol optical depth distributions over East Asia. Science China Earth Sciences 53, 1674–7313.

Holben, B.N., Tanré, D., Smirnov, A., Eck, T.F., Slutsker, I., Abuhassan, N., Newcomb, W.W., Schafer, J.S., Chatenet, B., Lavenu, F., Kaufman, Y.J., Vande Castle, J., Setzer, A., Markham, B., Clark, D., Frouin, R., Halthore, R., Karneli, A., O'Neill, N.T., Pietras, C., Pinker, R.T., Voss, K., Zibordi, G., 2001. An emerging ground based aerosol climatology: aerosol optical depth from AERONET. Journal of Geophysical Research 106, 12067–12097.

Huebert, B.J., Bates, T., Russell, P.B., Shi, G., Kim, Y.J., Kawamura, K., Carmichael, G., Nakajima, T., 2003. An overview of ACE-Asia: strategies for quantifying the relationships between Asian aerosols and their climatic impacts. Journal of Geophysical Research 108 (D23), 8633.

Ichoku, C., Chu, D.A., Mattoo, S., Kaufman, Y.J., Remer, L.A., Tanré, D., Slutsker, I., Holben, B.N., 2002. A spatio-temporal approach for global validation and analysis of MODIS aerosol products. Geophysical Research Letters 29, 8006–8010.

IPCC, 2007. Climate Change 2007: The Physical Science Basis. Cambridge University Press, New York. 131–216.

Kim, D., Sohn, B., Nakajima, T., Takamura, T., Takemura, T., Choi, B., Yoon, S., 2004. Aerosol optical properties over East Asia determined from ground-based sky radiation measurements. Journal of Geophysical Research 109, D02209.

Kim, S.W., Yoon, S.C., Kim, J., Kim, S.Y., 2007. Seasonal and monthly variations of columnar aerosol optical properties over East Asia determined from multi-year MODIS, LIDAR, and AERONET Sun/sky radiometer measurements. Atmospheric Environment 41 (8), 1634–1651.

Lei, Y., Zhang, Q., He, K.B., Streets, D.G., 2011. Primary anthropogenic aerosol emission trends for China, 1990–2005. Atmospheric Chemistry and Physics 11, 931–954.

Lelieveld, J., Crutzen, P.J., Ramanathan, V., Andreae, M.O., Brenninkmeijer, CA.M., Campos, T., Cass, G.R., Dickerson, R.R., Fischer, H., Gouw, J.A., de, Hansel, A., Jefferson, A., Kley, D., Laat, AT.J., de, Lal, S., Lawrence, M.G., Lobert, J.M., Mayol-Bracero, O.L., Mitra, A.P., Novakov, T., Oltmans, S.J., Prather, K.A., Reiner, T., Rodhe, H., Scheeren, H.A., Sikka, D., Williams, J., 2001. The Indian ocean experiment: widespread air pollution from South and South-East Asia. Science 291 (5506), 1031–1036.

Levy, R.C., Remer, L.A., Mattoo, S., Vermote, E.F., Kaufman, Y.J., 2007. Second generation operational algorithm: retrieval of aerosol properties over land from inversion of moderate resolution Imaging spectroradiometer spectral reflectance. Journal of Geophysical Research 112, D13211.

Levy, R.C., Leptoukh, G., Kahn, G.R., Zubko, V., Gopalan, A., Remer, L.A., 2009. A Critical Look at deriving monthly aerosol optical depth from satellite data. IEEE Transactions on Geoscience and Remote Sensing 47 (8), 2942–2956.

Levy, R.C., Remer, L.A., Kleidman, R.G., Mattoo, S., Ichoku, C., Kahn, R., Eck, T.F., 2010. Global evaluation of the Collection 5 MODIS dark-target aerosol products over Land. Atmospheric Chemistry and Physics 10, 10399–10420.

Li, Z., et al., 2007. Preface to special section: overview of the East Asian study of tropospheric aerosols: an international regional experiment (EAST-AIRE). Journal of Geophysical Research 112, D22S00.

Li, Z., Zhao, X., Kahn, R., Mishchenko, M., Remer, L., Lee, K.-H., Wang, M., Laszlo, I., Nakajima, T., Maring, H., 2009. Uncertainties in satellite remote sensing of aerosols and impact on monitoring its long-term trend: a review and perspective. Annales Geophysicae 27, 2755–2770.

Li, Z., 2004. Aerosol and climate: a perspective from East Asia. In: Observation, Theory, and Modeling of the Atmospheric Variability. World Scientific Publishing Company, pp. 501–525.

Lu, Z., Streets, D.G., Zhang, Q., Wang, S., Carmichael, G.R., Cheng, Y.F., Wei, C., Chin, M., Diehl, T., Tan, Q., 2010. Sulfur dioxide emissions in China and sulfur trends in East Asia since 2000. Atmospheric Chemistry and Physics 10, 6311–6331.

Matsui, H., Koike, M., Kondo, Y., Takegawa, N., Fast, J.D., Pöschl, U., Garland, R.M., Andreae, M.O., Wiedensohler, A., Sugimoto, N., Zhu, T., 2010. Spatial and temporal variations of aerosols around Beijing in summer 2006: 2. Local and column aerosol optical properties. Journal of Geophysical Research 115, D22207.

Menon, S., Hansen, J., Nazarenko, L., Luo, Y., 2002. Climate effects of black carbon aerosols in China and India. Science 297, 2250–2253.

Mishchenko, M.I., Geogdzhayev, I.V., 2007a. Satellite remote sensing reveals regional tropospheric aerosol trends. Optics Express 15, 7423–7438.

Mishchenko, M.I., Geogdzhaev, I.V., Rossow, W.B., Cairns, B., Carlson, B.E., Lacis, A.A., Liu, L., Travis, L.D., 2007b. Long-term satellite record reveals likely recent aerosol trend. Science 315, 1543.

Ohara, T., Akimoto, H., Kurokawa, J., Horii, N., Yamaji, K., Yan, X., Hayasaka, T., 2007. An Asian emission inventory of anthropogenic emission sources for the period 1980–2020. Atmospheric Chemistry Physics 7, 4419–4444.

Remer, L.A., Tanre′, D., Kaufman, Y.J., Ichoku, C., Mattoo, S., Levy, R., Chu, D.A., Holben, B.N., Dubovik, O., Ahmad, Z., Smirnov, A., Martins, J.V., Li, R.-R., 2002. Validation of MODIS aerosol retrieval over ocean. Geophysical Research Letters 29 (12), 8008.

Remer, L.A., Kaufman, Y.J., Tanré, D., Mattoo, S., Chu, D.A., Martins, J., Li, R.-R., Ichoku, C., Levy, R.C., Kleidman, R.G., Eck, T.F., Vermote, E., Holben, B.N., 2005. The MODIS aerosol algorithm, products, and validation. Journal of the Atmospheric Sciences 62 (4), 947–973.

Remer, L.A., Kleidman, R.G., Levy, R.C., Kaufman, Y.J., Tanré, D., Mattoo, S., Martins, J.V., Ichoku, C., Koren, I., Yu, H., Holben, B., 2008. Global aerosol climatology from the MODIS satellite sensors. Journal of Geophysical Research 113, D14S07.

Seinfeld, J.H., Carmichael, G.R., Arimoto, R., Conant, W.C., Brechtel, F.J., Bates, T.S., Cahill, T.A., Clarke, A.D., Doherty, S.J., Flatau, P.J., Huebert, B.J., Kim, J., Markowicz, K.M., Quinn, P.K., Russell, L.M., Russell, P.B., Shimizu, A., Shinozuka, Y., SongCh, H., Tang, Y., Uno, I., Vogelmann, A.M., Weber, R.J., Woo, J., Zhang, X.Y., 2004. ACE-ASIA: regional climatic and atmospheric Chemical effects of Asian dust and pollution. Bulletin of the American Meteorological Society 85 (3), 367–380.

Sheng, L., Guo, Zh, Gao, H., 2005. Preliminary study on Element composition and source apportionment of atmospheric aerosol over Bohai Sea. Environmental Monitoring in China 21 (1), 16–20 (in Chinese).

Streets, D.G., Aunan, K., 2005. The importance of China's household sector for black carbon emissions. Geophysical Research Letters 32, L12708.

Streets, D.G., Gupta, S., Waldhoff, S.T., Wang, M.Q., Bond, T.C., Bo, Y., 2001. Black carbon emissions in China. Atmospheric Environment 35, 4281–4296.

Streets, D.G., Carmichael, G.R., Fernandes, S.D., Fu, Q., He, D., Klimont, Z., Nelson, S.M., Tsai, N.Y., Wang, M.Q., Woo, J.-H., Yarber, K.F., 2003. An inventory of gaseous and primary aerosol emissions in Asia in the year 2000. Journal of Geophysical Research 108 (D21), 8809.

Streets, D.G., Bond, T.C., Lee, T., Jang, C., 2004. On the future of carbonaceous aerosol emissions. Journal of Geophysical Research 109, D24212.

Streets, D.G., Wu, Y., Chin, M., 2006. Two-decadal aerosol trends as a likely explanation of the global dimming/brightening transition. Geophysical Research Letters 33, L15806.

Tian, H., Ma, J., Li, W., Liu, H., 2005. Simulation of forcing of sulfate aerosol on direct radiation and its climate effect over middle and eastern China. Journal of Applied Meteorological Science 16 (3), 322–333 (in Chinese).

Wang, Y., Che, H., Ma, J., Wang, Q., Shi, G., Chen, H., Goloub, P., Hao, X., 2009. Aerosol radiative forcing under clear, hazy, foggy, and dusty weather conditions over Beijing, China. Geophysical Research Letters 36, L06804.

Wang, Y., Xin, J., Li, Z., Wang, S., Wang, P., Hao, W. M., Nordgren, B. L., Chen, H., Wang, L. and Sun, Y. Seasonal variations in aerosol optical properties over China, Journal of Geophysical Research, doi:10.1029/2010JD015376, in press.

Xiao, H., Gregory, R.C., Zh, Yang, 1998. A modelling evaluation of the impact of mineral aerosols on the particulate sulfate formation in East Asia. Scientia Atmospherica Sinica 22 (3), 343–353 (in Chinese).

Xin, J., Wang, Y., Li, Z., Wang, P., Hao, W.M., Nordgren, B.L., Wang, S., Liu, G., Wang, L., Wen, T., Sun, Y., Hu, B., 2007. AOD and Angstrom wavelength exponent of aerosols observed by the Chinese sun hazemeter Network from August 2004 to September 2005. Journal of Geophysical Research 112, D05203.

Xin, J., Wang, Y., Li, Z., Wang, P., Wang, S., Wen, T., Sun, Y., 2006. Introduction and calibration of the Chinese sun hazemeter Network. Environmental Science 27 (9), 1697–1702 (in Chinese).

Xin, J., Du, W., Wang, Y., Gao, Q., Li, Z., Wang, M., 2010a. Aerosol optical properties affected by a strong dust storm in Central and Northern China. Advances in Atmospheric Sciences 27 (3), 562–574.

Xin, J., Wang, Y., Tang, G., Wang, L., Sun, Y., Wang, Y., Hu, B., Song, T., Ji, D., Wang, W., Li, L., Liu, G., 2010b. Variability and reduction of atmospheric pollutants in Beijing and its surrounding area during the Beijing 2008 olympic games. Chinese Science Bulletin 55 (18), 1937–1944.

Yan, X., Ohara, T., Akimoto, H., 2006. Bottom-up estimate of biomass burning in mainland China. Atmospheric Environment 40, 5262–5273.

Yu, X., Zhu, B., Zhang, M., 2009. Seasonal variability of aerosol optical properties over Beijing. Atmospheric Environment 43, 4095–4101.

Zhang, J., Reid, J.S., 2010. A decadal regional and global trend analysis of the aerosol optical depth using a data-assimilation grade over-water MODIS and level 2 MISR aerosol products. Atmospheric Chemistry and Physics 10, 10949–10963.

Zhao, TX.-P., Laszlo, I., Guo, W., Heidinger, A., Cao, C., Jelenak, A., Tarpley, D., Sullivan, J., 2008. Study of decadal trend in aerosol optical thickness observed from operational AVHRR satellite instrument. Journal of Geophysical Research 113, D07201.

Zheng, M., Salmon, L.G., Schauer, J.J., Zeng, L., Kiang, C.S., Zhang, Y., Cass, G.R., 2005. Seasonal trends in PM2.5 source contributions in Beijing. China. Atmospheric Environment 39, 3967–3976.

Zhou, R., Liu, H., Jiang, W., 2004. The study on the transport of dust aerosol in China. Scientia Meteorologica Sinica 24 (1), 16–25 (in Chinese).